Soil salinization affected by hydrogeochemical processes of shallow groundwater in Cangzhou City, a coastal region in North China

Jin He, Qijun Den, Xuejun Ma, Xiaosi Su and Xuemei Ma

ABSTRACT

This study sought to further the current understanding on the relationship between soil salinization and groundwater hydrochemical processes. To this effect, 33 soil samples and 64 shallow groundwater samples were collected in Cangzhou City, a coastal region of the North China Plain. Soil salinization showed clear patterns of zonation from inland to coastal areas. The no-salinization or mild-salinization with Cl-SO_4 or SO_4-Cl types were discovered in the west of Cang County farther from the sea; this was restricted by brackish groundwater with HCO_3·SO_4-Ca·Na type and the deep water table. With increasing proximity to the coastline, groundwater salinity increased soil salt content and salinization, the effects of which were mainly determined by specific Cl/Br ratios and the seawater mixing index in groundwater. The positive $\delta^{18}O$ and $\delta^{2}H$ content in groundwater was related to the strong evaporation of groundwater with a shallow water table, indicating that the high soil salinity directly affected relict seawater evaporation. The observed severe-salinization soil and high NO_3^- concentrations indicate that agricultural activities were non-negligible salt sources in areas close to the sea. The results have relevance in improving saline-alkali soil and utilization of soil resources in the coastal areas in the North China Plain.

Key words | Cangzhou, geochemistry, groundwater, isotopes, soil salinization

Jin He (corresponding author)
College of New Energy and Environment,
Jilin University,
Changchun 130021,
China
E-mail: *hejing007105@126.com*

Jin He
Qijun Den
Xuejun Ma
Xuemei Ma
Center for Hydrogeology and Environmental Geology,
China Geological Survey,
Baoding 071051,
China

Jin He
Xiaosi Su
Institute of Water Resources and Environment,
Jilin University,
Changchun 130026,
China

Xiaosi Su
College of Construction Engineering,
Jilin University,
Changchun 130021,
China

HIGHLIGHTS

- Strong zonation was evident in soil salinization from east to west in Cangzhou area.
- Soil salinity was restricted by shallow groundwater salinization in coastal area.
- The highest soil salinity was driven by strong evaporation of relict seawater.

INTRODUCTION

Soil salinization is currently one of the most important global environmental issues. Approximately 3.31×10^8 ha of land is threatened by salinization; this equates to over 10% of the total irrigated land area worldwide (Ghassemi *et al.* 1995). Soil salinization is now increasing in severity in the United States, Pakistan, China, Argentina, Sudan, and many countries in Central and Western Asia. In China, salinized soils span approximately 3.6×10^7 ha, accounting for 4.88% of the total available land in the country. More than a third of this land is located in coastal areas, spanning a total area exceeding 15×10^6 ha (Wang *et al.* 2016).

Soil salinization in coastal areas is influenced by climate, groundwater, soil texture, and other abiotic factors, and uncontrolled human activities. Groundwater salinity and

doi: 10.2166/nh.2021.183

levels are considered critical factors influencing soil salinization. Uma (2013) observed that saline soil is typically situated in relatively low areas with shallow groundwater and a low groundwater hydraulic gradient in the Nam Kam River basin. Wang *et al.* (2015a, 2015b) demonstrated that climatic factors, salinity, shallow groundwater depth, and vegetation on soil surface are important factors impacting on soil salinization in the coastal area of Tianjin. Lu *et al.* (2017) reported that the salt content of soil is closely related to the hydrochemical characteristics of groundwater in the Yellow River Delta. As high capillary rise occurs in silty clay soils from marine deposition, soil salt is prone to accumulating on the soil surface from capillary water evaporation in coastal areas.

Cangzhou is a typical coastal city east of the North China Plain (NCP), characterized by flood and coastal plains with extensive shallow saline water. The land in this region has long been affected by seawater intrusion alongside uncontrolled agricultural irrigation patterns. As such, a large amount of salt has accumulated on the soil surface; in the 1950s, this spanned an area exceeding 3,000 km^2 (Chen *et al.* 2018). Since the late 1970s, the over-exploitation of deep confined water to satisfy increased agricultural water demand has led to a decline in the shallow groundwater level, decreasing the area impacted by high soil salinity. However, the soil salinization problem continues to be a serious issue in the present day; saline soil currently spans an area of 1,820 km^2, accounting for 62.1% of the total area of the coastal region (Chen *et al.* 2018).

The long-term influence of seawater intrusion, groundwater mineralization and soil salinization has become inevitable in coastal areas. In terms of soil salinization, few studies have focused on the spatial distribution pattern (Wang *et al.* 2015a, 2015b), origin and controlling factors (Zhou *et al.* 2012), and reclamation of saline soils (Liu 2018) in the NCP at regional scales. There has been an absence of research on the relationship between soil salinity and groundwater salinization in the Cangzhou area. To understand soil salinization mechanisms involving shallow groundwater hydrogeochemical processes, and aid the reasonable use of land resources in coastal areas, this study sought to address three key objectives: (1) to delineate the existing soil salinity distribution and characterize soil salinization and shallow groundwater hydrochemistry in coastal areas; (2) to discuss the origin of soil salinity and its relationship with hydrogeochemical factors; and (3) to improve the current understanding of soil salinization by controlling shallow groundwater salinity accumulation processes. This study provides insights into the distribution and origin of soil salinity under shallow groundwater salinization conditions in coastal areas.

STUDY AREA

The study area is located in the coastal plain of Cangzhou City and spans approximately 4,350 km^2; this is subordinate to Cang County and Huanghua City (Figure 1). The elevation in the study area is generally within 5–10 m above mean sea level (m.s.l.), declining from the north, and from the west toward Bohai Bay in the east. The region has a continental monsoon climate with an annual average air temperature of 12.2 °C, an average annual precipitation of approximately 586.5 mm, and an evaporation of 1,864.5 mm/y. Approximately 78% of precipitation occurs during the rainy season between July and August.

The groundwater system is classified into four aquifers based on the geological period; Holocene, Late Pleistocene, Middle Pleistocene, and Early Pleistocene. Unconfined shallow aquifers refer to aquifers with burial depths lower than 30 m that are associated with the Holocene and Late Pleistocene formations. Thee aquifers are separated by silt and sandy gravel, and medium-fine sand. Meteoric water is the main source of shallow groundwater and evaporation, being prone to manual exploitation; leakage into deeper confined aquifers is its main means of discharge.

The variation in shallow groundwater depth fluctuates between 0.5 and 5 m from east to west (Figure 1). The highest water table occurs during the rainy season, while the lowest water table occurs in spring because of the high evaporation and low precipitation recharge. Groundwater also flows locally from west to east, where hydraulic gradients range between 1/3,000 and 1/5000.

MATERIALS AND METHODS

Sampling and chemical analysis

To understand the origin and evolution of soil salinity in the study area, 33 surface soil samples (at depths of 0–20 cm)

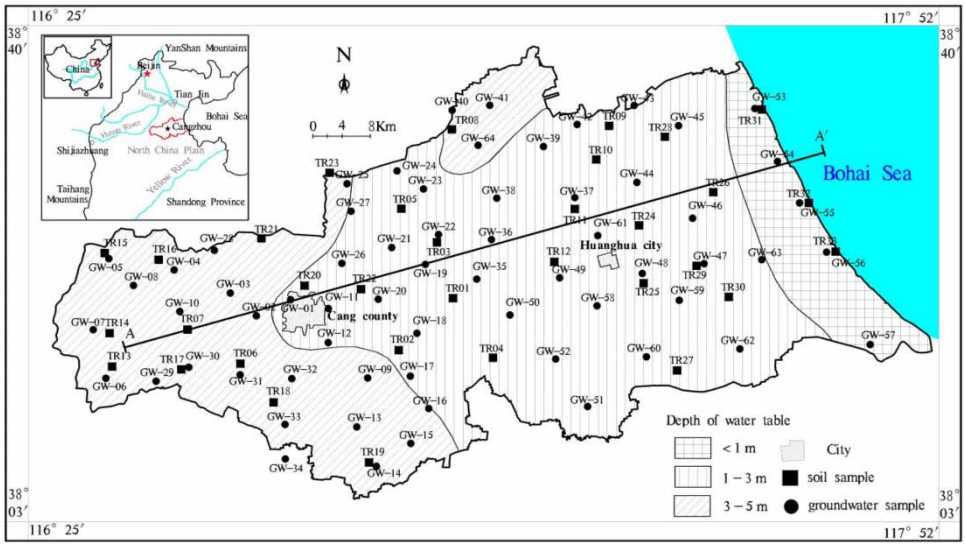

Figure 1 | Location of soil and shallow groundwater sampling points. The oblique line represents the different groundwater depths. The A-A′ line indicates hydrogeological profile with Figure 11.

were collected from the study area in September 2014. Sampling points were evenly distributed across the farmland. Soil samples were obtained from three sub-samples mixed over a distance of 30 m, resulting in a sample mass of approximately 1.5–2.0 kg, representing an artificial environment. Additionally, 64 groundwater samples in the phreatic aquifer at a depth of 2–20 m were collected; these were uniformly distributed throughout the study area. To ensure that each sample was representative of the chemical characteristics of groundwater, samples were collected using peristaltic pumps after ensuring constant conductivity and redox potential.

Soil samples were prepared via air drying and lapping, and then passed through a 2 mm sieve to remove small stones and plant roots. The most abundant ions contained in each soil sample were measured via extraction from a sample that had a soil to distilled water ratio of 1:5 ratio, excluding carbon dioxide. The concentrations of cations (i.e. Ca^{2+}, Mg^{2+}, Na^{+}, K^{+}), were determined using an atomic absorption spectrometer (Analytikjena ContrAA 300,Germany), concentrations of CO_3^- and HCO_3^- were determined using titration, and the concentrations of anions (Cl^-, SO_4^{2-}, NO_3^-, Br^-) were measured via ion chromatography (Thermo Scientific Dionex ICS-1100, USA). The salt content (SC) was defined as the sum of anions and cations. The extremely low bromine concentrations in soil-soluble salts meant that only 11 soil sample analysis results were obtained using the detection limit of bromine.

For cation analyses, groundwater samples were filtered through 0.45 μm membrane filters and acidified to pH < 2 with analytical-grade HNO_3. Alkalinity was measured via titration on the day samples were collected. The method used to determine the concentration of ions (i.e. Na^{+}, K^{+}, Ca^{2+}, Mg^{2+}, Cl^-, Br^-, F^-, NO_3^-, SO_4^{2-}) in groundwater was the same as that utilized in soil. Total dissolved solids (TDS) were calculated as the sum of ion concentrations. Major ions in the soil and groundwater samples were determined at the Geological Experiment Testing Center of Hebei Province. Analytical precision and accuracy were estimated to be better than 5% for all major ions based on repeated analyses of samples and standard solutions. The $\delta^{18}O$ and $\delta^{2}H$ stable isotopes in groundwater were measured via mass spectrometry (Finnigan MAT 253, USA) at the Institute of Hydrogeology and Environmental Geology, Chinese Academy of Geological Sciences. The $\delta^{18}O$ and $\delta^{2}H$ values were expressed relative to international standards (V-SMOW for ^{18}O and ^{2}H), expressed as ‰. The analytical precision was ±1‰ for $\delta^{2}H$ and ±0.2‰ for $\delta^{18}O$.

Data analysis

Hydrochemical data was interpreted numerically and graphically through statistical analysis, correlation analysis, a piper diagram, and binary diagrams. SPSS software

(version 16.00) was used to determine the statistical correlation between anions and cations in soil and groundwater. AquaChem (version 3.7) was used to produce scatter and piper diagrams. The mineral saturation indices (SIs) of soil solutions and groundwater were calculated using PHREEQC software (version 2.17), used to verify the potential for mineral dissolution.

Calculation of seawater mixing index

The seawater mixing index (SMI), an index originally developed by Park *et al.* (2005), was used to determine the extent to which seawater and groundwater were mixing. It is premised on the construction of a function using the ratios of concentration proportions of Na, Mg, Cl, and SO_4 in groundwater to those of seawater. We used the SMI to evaluate the impact of saline water on soil salinization; the SMI was calculated using Equation (1):

$$SMI = a \times \frac{C_{Na}}{T_{Na}} + b \times \frac{C_{Mg}}{T_{Mg}} + c \times \frac{C_{Cl}}{T_{Cl}} + d \times \frac{C_{SO_4}}{T_{SO_4}} \quad (1)$$

where constants $a = 0.31$, $b = 0.04$, $c = 0.57$, $d = 0.08$ denote the relative concentrations of Na, Mg, Cl, and SO_4 in seawater, respectively; C is the objective concentration in mg/L; and T represents the regional threshold of the ions under consideration. Cumulative frequency curves were used to determine regional threshold values. If the SMI exceeds 1, this may indicate that groundwater is affected by seawater mixing (Park *et al.* 2005).

RESULTS

Distribution and types of soil salinization

The scatter plot illustrates the SC in soil, exhibiting a trend from high to low with increasing distance from the coastline (Figure 2). Nearly 24.2% of the soil samples had already progressed to a level at or exceeding moderate salinization (Table 1). The area with the highest soil content was largely distributed to the east of Huanghua City, in close proximity to the Bohai Sea. Approximately 33.3% of soil sample points exhibited non-salinization and mild-salinization; these were scattered mainly in Cang County. These results are similar to the soil contents in the low plains around the Bohai Sea (Zhou & Zhao 2015). The same patterns as soil salinity were also observed for the TDS of shallow groundwater; the TDS concentration increasing with proximity to the coastline. The TDS (maximum value = 30.95 g/L) of groundwater near the coast shared similarities with the salinity of the Bohai Sea (Li 1994).

The chemical types of salinization may be categorized into four types based on the Cl^-/SO_4^{2-} ratio in soil (Table 1). With decreasing distance to the coast, the soil salinity ranges from a sulfate to chloride–sulfate type, and sulfate–chloride to chloride type. Most non-salinized soil samples contained the chloride–sulfate and sulfate types, while most soil samples with severe salinization were of the chloride type. The maximum Cl^-/SO_4^{2-} and SC in the soils were 74.42 and 7.53 g/kg, respectively, because of low sulfate and high chloride concentrations.

Hydrochemical characteristics of soil and shallow groundwater

The piper diagram illustrates the hydrochemistry of soluble salt in soil and groundwater; it ranges from no salinization to severe salinization, and brackish to brine water, respectively (Figure 3). The hydrochemical types of soluble salts corresponding to varying extents of soil salinization significantly differ. The key anions in non-saline and slightly saline soil were HCO_3^- and SO_4^{2-}, accounting for more than 60% of anions. Cl^- was the major anion in severely saline soil, accounting for 80% of total anions, while Na^+ was the dominant cation in severely saline soils. The most abundant anions present in the severely saline soils included chloride, phosphate, and sulfate; the chloride ions had the highest concentration. The hydrochemical type of groundwater switched from HCO_3·SO_4–Ca·Na and SO_4·HCO_3–Na·Ca to the Cl–Na type with an increase in salinity. Sample points with severe salinization and brine water were close to that of seawater, showing that soil and groundwater near the coast are more frequently influenced by seawater.

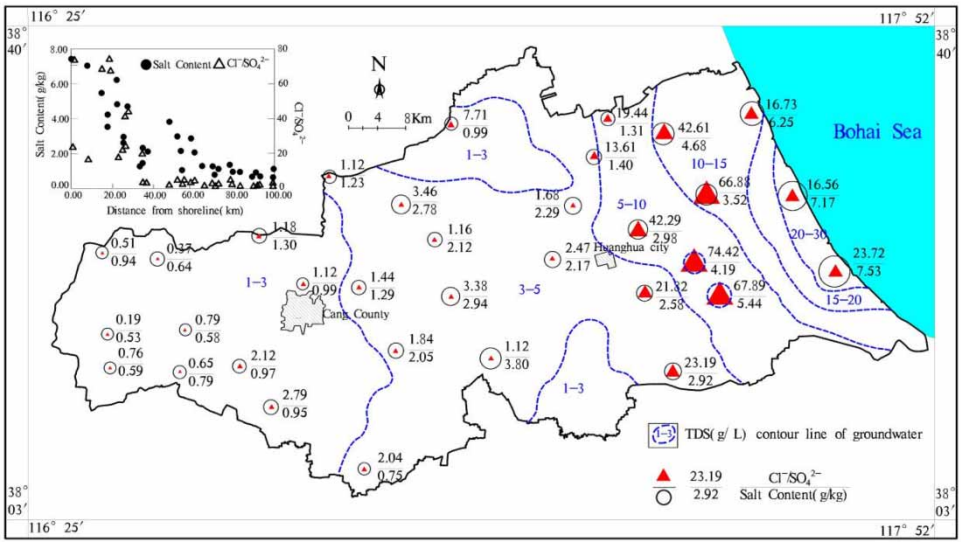

Figure 2 | Distribution of soil salt content and computed Cl^-/SO_4^{2-} for soils in the study area; the blue broken line represents the TDS contour value in groundwater. Inset: scatter plots of salt content and Cl/SO_4^{2-} with respect to distance from shoreline. Please refer to the online version of this paper to see this figure in colour: http://dx.doi.org/10.2166/nh.2021.183.

Table 1 | The extent and types of soil salinization

Salinization extent	Salt content ($g \cdot kg^{-1}$)	Salinization type	Cl^-/SO_4^{2-}
No salinization	<1.0	Sulfate type	<0.5
Mild salinization	1.0–3.0	Chloride–sulfate type	0.5–1.0
Moderate salinization	3.0–6.0	Sulfate–chloride type	1.0–4.0
Severe salinization	6.0–10.0	Chloride type	>4.0
Saline soils	>10.0	Sulfate type	–

Note: The extent and type of soil salinization in this study were based on this table. The former was based on the salinization classification criteria for the Second Agricultural Soil Survey in China.

Statistical analysis of soil salinity and shallow groundwater

Table 2 summarizes the basic statistics relating to the hydrochemical parameters for soluble salts in soils and shallow groundwater. As a result of influences from primary geology and anthropogenic activity, most parameters exhibited an increase in SC. All major cations and anions were present in wide-ranging concentrations with high standard deviations. For example, the pH of the soils was alkaline, averaging 7.75, and the soil SC spanned a range between 0.58 and 7.53 g/kg (mean value = 2.48 g/kg), indicating a moderate degree of salinization (Table 1). The coefficients of variation for Na and Cl ions in soil were also high, at 0.95 and 1.18, respectively, indicating substantial variability among halites for soil salinity in the study area. The high potassium concentrations (mean value = 0.43 mmol/L) and nitrate concentrations (mean value = 0.71 mmol/L) in soil are typical of farmlands located in proximity to coastal areas. The accumulation of nitrate in soils is a direct effect of the heavy use of N fertilizers in the NCP.

In groundwater, the pH ranged from 6.08 to 8.27, with a median of 7.28; this is slightly lower than the pH of soil. TDS varied between 1.07 and 30.95 g/L, averaging 5.29 g/L, indicating an upward trend in groundwater salinization which is a relatively serious issue. The mean concentrations of Na^+ and Cl^- were 52.72 and 65.01 mmol/L, respectively; this equates to twice that observed in the soils. The high concentrations of these ions in groundwater samples suggest that saline water has mixed with groundwater. There was considerable variation in the concentrations of K^+ and NO_3^-, ranging from 0.01 to 12.92 mmol/L, and 0.02 to 11.78 mmol/L, and averaging of 1.31 and 1.41 mmol/L, respectively. This reflects a considerable deterioration in groundwater quality as a result of seawater intrusion and anthropogenic-induced contamination. The standard deviations and coefficients of variation were high for different anions and cations in shallow groundwater, reflecting the

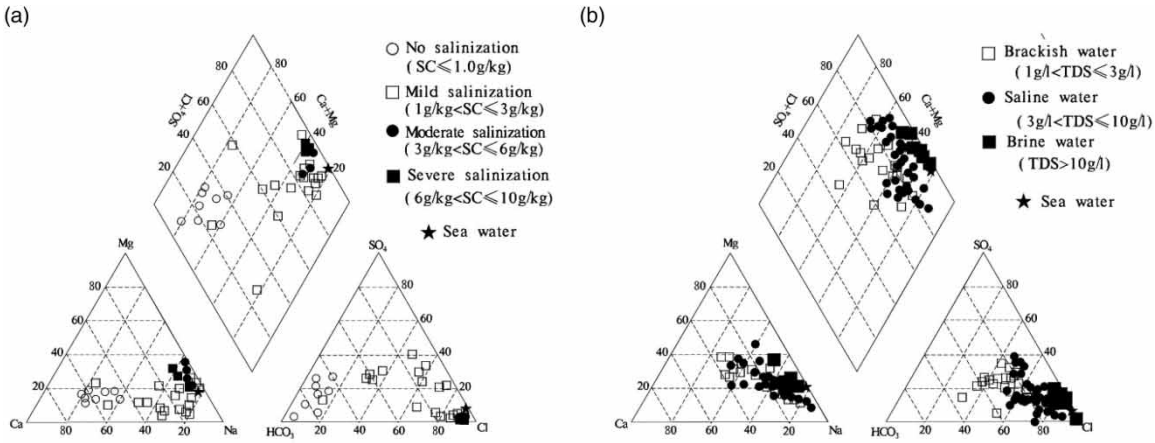

Figure 3 | Piper diagram of soluble salt in (a) soil; and (b) shallow groundwater. The degree of soil salinization was classified based on Table 1. The groundwater was classified according to the total dissolved solids concentration for brackish water (1–3 g/L), saline water (3–10 g/L), and brine water (>10 g/L).

Table 2 | Descriptive statistical parameters of water-soluble ions in soil and shallow groundwater

Item		pH	SC or TDS (g/kg)	HCO_3^- (mmol/l)	Cl^- (mmol/l)	SO_4^{2-} (mmol/l)	NO_3^- (mmol/l)	Br^-[a](mmol/l)	Ca^{2+} (mmol/l)	Mg^{2+} (mmol/l)	K^+ (mmol/l)	Na^+ (mmol/l)
Soil ($n = 33$)	Mean	7.75	2.48	6.62	29.08	2.00	0.71	0.11	2.90	4.42	0.44	24.10
	SD	0.34	1.93	4.90	34.24	1.87	0.64	0.04	2.68	5.53	0.64	22.85
	CV	0.04	0.79	0.40	1.18	0.93	0.90	0.39	0.56	1.25	1.46	0.95
	Min	7.12	0.58	1.88	0.36	0.14	0.02	0.03	0.53	0.35	0.02	1.59
	Max	8.50	7.53	31.34	116.25	6.56	2.27	0.17	15.92	18.91	3.15	89.43
Groundwater ($n = 64$)	Mean	7.28	5.29	10.11	65.01	7.59	1.30	0.13	5.91	12.14	1.41	52.72
	SD	0.28	5.30	3.81	83.82	6.78	2.18	0.12	3.67	12.76	3.00	60.50
	CV	0.04	1.01	0.38	1.29	0.89	1.67	0.91	0.62	1.05	2.13	1.15
	Min	6.80	1.07	1.87	6.30	0.27	0.02	0.03	1.29	1.74	0.01	1.83
	Max	8.27	30.95	19.44	506.18	30.15	11.78	0.83	9.82	62.58	12.92	370.89

Note: Mean = arithmetic mean value; SD = standard deviation; CV = coefficient of variation; Min = minimum value; Max = maximum value.
[a]The value of bromine was based on 11 analyzed soil samples.

same regularity observed in the soil samples. This result suggests that the chemical composition of groundwater and soils is influenced by multiple sources and complex hydrochemical processes.

Hydrogen and oxygen isotopes in shallow groundwater

Table 3 presents a statistical summary of δ^2H and $\delta^{18}O$ stable isotopes for different levels of groundwater salinity. The $\delta^{18}O$ of brackish groundwater ranged from −9.1 to −6.2‰ (median value = −8.2‰), while the δ^2H of brackish groundwater ranged from −65.6 to −49.5‰ (median value = −60.4‰). The low standard deviation and coefficient of variation for $\delta^{18}O$ and δ^2H in brackish groundwater indicate that these groundwater samples with low TDS have a relatively stable recharge. In saline groundwater, the δ^2H ranged from −66.3 to −34.8‰ (median value = −55.8‰), while the $\delta^{18}O$ ranged from −9.1 to −3.3‰ (median value = −7.5‰). The δ^2H and $\delta^{18}O$ in brine groundwater were higher than those in saline and brackish groundwaters, with medians of −18.5 and 1.1‰, respectively. The coefficient of variation or δ^2H compared to that of $\delta^{18}O$ in brine water was relatively high (the coefficient of variation was 698.3 and 158.1%, respectively). This suggests that these parameters exhibit strong variation and shallow groundwater salinization is regulated by different hydrogeochemical processes including groundwater evaporation and seawater intrusion.

Table 3 | Statistical parameters of hydrogen and oxygen stable isotope data for different groundwater salinities

Water type		$\delta^{18}O$ (‰)	$\delta^{2}H$ (‰)
Brackish groundwater ($n = 22$)	Mean	−8.2	−60.4
	SD	0.66	3.70
	CV(%)	8.3	6.5
	Min	−9.1	−65.6
	Max	−6.2	−49.5
Saline water ($n = 35$)	Mean	−7.5	−55.8
	SD	1.43	7.41
	CV(%)	21.1	13.2
	Min	−8.9	−66.3
	Max	−3.3	−34.8
Brine water ($n = 7$)	Mean	1.1	−18.5
	SD	7.09	29.27
	CV(%)	698.3	158.1
	Min	−7.2	−55.4
	Max	11.8	22.1

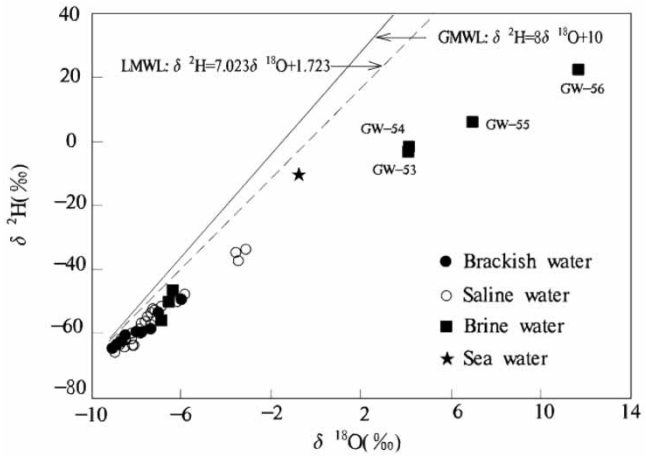

Figure 4 | Plot of $\delta^{2}H$ versus $\delta^{18}O$ for shallow groundwater based on groundwater salinity, compared with the local meteoric water line (LMWL) of the North China Plain (Zhang et al. 2000).

The $\delta^{2}H$ versus $\delta^{18}O$ relationship in Figure 4 shows that most brackish and brine groundwater plots are close to the local meteoric water line (LMWL; $\delta^{2}H = 7.023\delta^{18}O + 1.723$) and global meteoric water line (GMWL; $\delta^{2}H = 8\delta^{18}O + 10$). This is indicative of their meteoric origin, and implies that modern rainfall is the dominant component of shallow groundwater. The partial groundwater points of saline and brine with less negative or positive $\delta^{2}H$ and $\delta^{18}O$ values (−2.3 to 22.1 and −4.2 to 11.8‰, respectively; sample: GW-53–GW-56) fall to the right of the LMWL. This signifies that these points were subjected to seawater evaporation, as these samples were collected at a shallow depth (i.e. well depth below 2 m), within reclaimed land from the sea approximately 30 years ago.

To illustrate the relationships between different ionic species in soil and groundwater, Tables 4 and 5 outline the correlation coefficients between the major ions using Spearman's correlation analysis. The coefficient matrices for soil and groundwater were compared for SC or TDS between Na^{+}, Mg^{2+}, and Cl^{-}, with a high positive correlation (>0.75) at $p < 0.05$. The high correlation implies that the soil and groundwater salinities were largely controlled by these ions. Bromine is an indicator ion in seawater, as opposed to naturally occurring groundwater and soil water. The Pearson correlation matrix of Tables 4 and 5 show that Br^{-} is strongly correlated with Na^{+}, Mg^{2+}, Cl^{-}, SC and TDS in soil and groundwater, highlighting that soil and groundwater originate from the same marine source.

DISCUSSION

Genesis and evolution of soil solutes

In general, the ion ratio method is used to distinguish the source of constituents in the target solution. Figure 5 shows the evolution of chemical element concentrations in the soils and groundwater sampled from the study area. Most ionic ratio distributions in soil samples were consistent with those of groundwater samples. This signifies that the origins of ions between soil and groundwater were similar in terms of involving the same hydrogeochemical processes.

For the majority of samples, the Na/Cl ratio had gradually decreased with an increase in the Cl^{-} concentration (Figure 5(a)). When the Cl^{-} concentration is less than 37 mmol/L, the Na/Cl ratio for soil samples in the study area generally exceeds 1. Its comparability with the seawater ratio (0.85) (Han *et al.* 2015) may be attributable to silicate weathering reactions in continental sediments. The others are plotted around the seawater ratio line with increasing Cl^{-} in the soil. Seawater intrusion may be responsible for the chloride concentration.

Based on the comparison of the Mg/Cl ratio versus Cl^{-} (Figure 5(b)) with the Na/Cl ratio versus Cl^{-}, both laws are

Table 4 | Spearman's correlation matrix of the hydrochemical parameters of soil samples

	pH	SC	Na^+	K^+	Ca^{2+}	Mg^{2+}	Cl^-	SO_4^{2-}	HCO_3^-	NO_3^-	Br^-
pH	1										
SC	0.077	1									
Na^+	0.061	0.984**	1								
K^+	0.045	0.812**	0.771**	1							
Ca^{2+}	0.14	−0.131	−0.191	−0.227	1						
Mg^{2+}	0.132	0.860**	0.819**	0.762**	−0.118	1					
Cl^-	0.104	0.977**	0.982**	0.775**	−0.186	0.835**	1				
SO_4^{2-}	−0.171	0.349*	0.334	0.378*	0.281	0.302	0.286	1			
HCO_3^-	−0.081	−0.232	−0.277	−0.066	0.124	−0.105	−0.326	−0.295	1		
NO_3^-	−0.031	0.581**	0.568**	0.471**	0.103	0.660**	0.544**	0.483**	−0.206	1	
Br^-	0.364	0.761**	0.800**	0.664*	0.027	0.800**	0.845**	−0.055	0.709*	0.409	1

Note: The value of bromine was based on 11 analyzed soil samples.
*Correlation is significant at the 0.05 level.
**Correlation is significant at the 0.01 level.

Table 5 | Spearman's correlation matrix of the hydrochemical parameters of groundwater samples

	pH	TDS	Na^+	K^+	Ca^{2+}	Mg^{2+}	Cl^-	SO_4^{2-}	HCO_3^-	NO_3^-	Br^-
pH	1										
TDS	−0.008	1									
Na^+	0.211	0.903**	1								
K^+	0.217	0.587**	0.634**	1							
Ca^{2+}	−0.509**	0.572**	0.260*	0.249*	1						
Mg^{2+}	−0.297*	0.819**	0.583**	0.346**	0.819**	1					
Cl^-	0.00	0.970**	0.911**	0.614**	0.527**	0.753**	1				
SO_4^{2-}	−0.03	0.519**	0.354**	0.174	0.613**	0.706**	0.382**	1			
HCO_3^-	−0.223	−0.019	0.085	−0.091	−0.306*	−0.112	−0.051	−0.244	1		
NO_3^-	−0.044	−0.208	−0.216	−0.04	−0.037	−0.181	−0.250*	−0.042	0.049	1	
Br^-	−0.05	0.851**	0.770**	0.483**	0.581**	0.744**	0.872**	0.437**	−0.081	−0.192	1

Note: *Correlation is significant at the 0.05 level.
**Correlation is significant at the 0.01 level.

similar. When the Cl^- content was greater than 45 mmol/L in soil, the molar relationship Mg/Cl (0.178) was similar to that of seawater (0.2) (Neal & Kirchner 2000). The predominance of Mg^{2+} and Cl^- may be attributed to the proximity to the sea, enabling sea spray and ongoing seawater intrusion to impact nearby soils.

Figure 5(c) shows the abundance of $Ca^{2+} + Mg^{2+}$ cations over HCO_3^- in soil and groundwater. Approximately 60% of soil samples and most groundwater samples fell above the 1:2 trend line; this suggests Ca^{2+} input from Na-Ca exchange and meteoric contribution from gypsum. This observation, combined with Figure 6(a) and 6(b) where the $SI_{calcite}$ and $SI_{dolomite}$ exceeded zero, indicate a state of super-saturation in terms of a particular mineral. These values decreased with increasing chloride concentration, indicating calcite precipitation with increasing Ca, attributable to calcite solubility control.

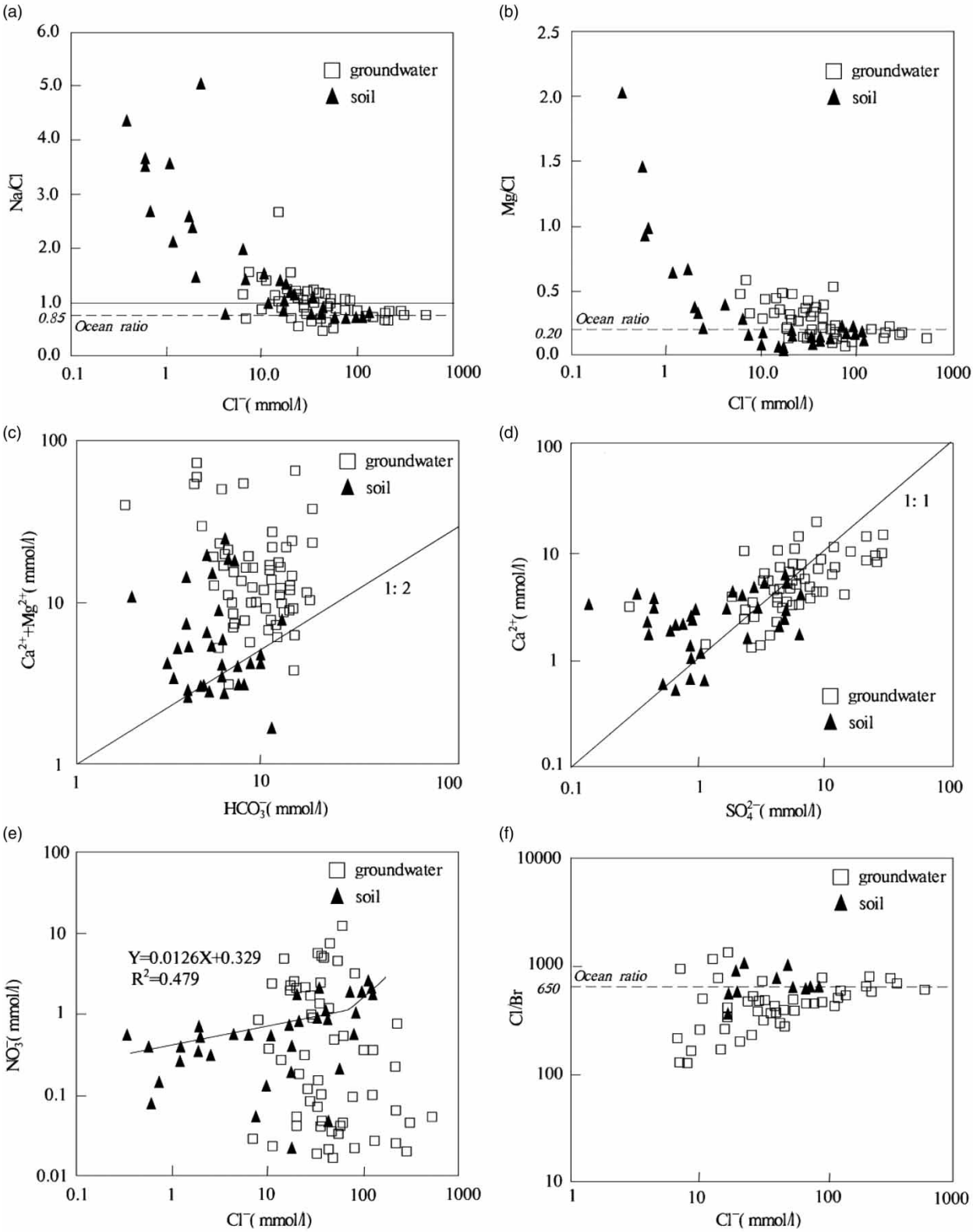

Figure 5 | Relationships between various chemical properties in groundwater and soil: (a) Na/Cl versus Cl^-; (b) Mg/Cl versus Cl^-; (c) $Ca^{2+} + Mg^{2+}$ versus HCO_3^-; (d) Ca^{2+} versus SO_4^{2-}; (e) NO_3^- versus Cl^-; and (f) Cl^-/Br^- versus Cl^-. The dashed line depicts the ratio of related ions in seawater.

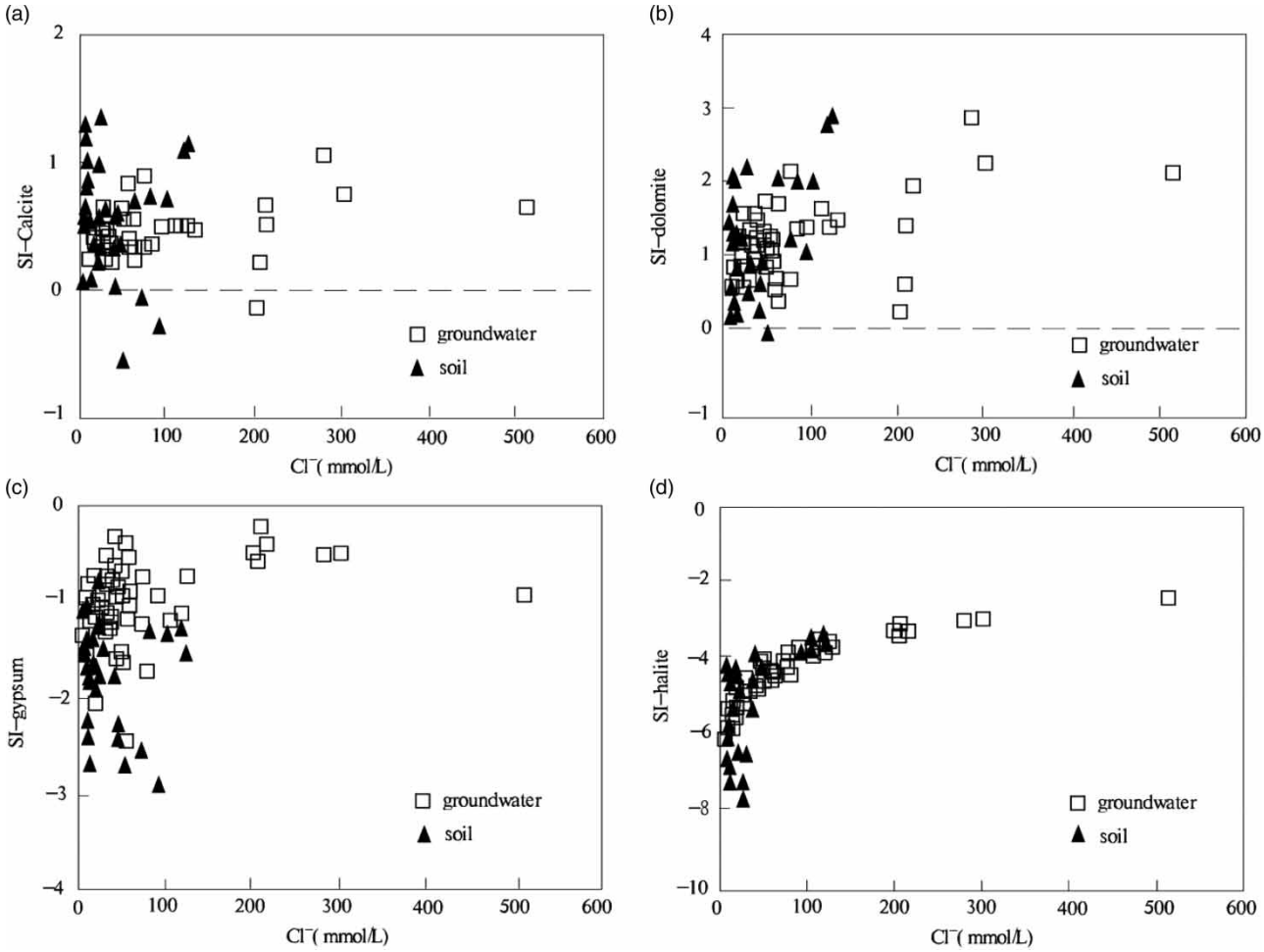

Figure 6 | Relationships between Cl^- concentration and the calculated saturation indices of soluble salt in soil and groundwater.

The scatter plots of Ca^{2+} against SO_4^{2-} in Figure 5(d) had a relationship that was roughly 1:1, suggesting that these ions in soil and groundwater samples had originated from the dissolution of gypsum. In terms of the increase in chloride ions, all soil samples were undersaturated with respect to gypsum (Figure 6(c)). This indicates favorable conditions for sulfate dissolution in soil salinization processes. A previous study reported that the parent material of soil in the study area originated from weathered alluvial deposits of the Taihang Mountains; these are good sources of sulfur (Chen *et al.* 2003). The dissolution of sulfate minerals, such as gypsum and anhydrite, during water–rock interactions is considered to be a hydrogeochemical process that regulates sulfate content in soil and groundwater.

Nitrate in soil and groundwater is largely derived from chemical fertilizers and domestic sewage. Figure 5(e) shows that in the soil samples there was a weak positive correlation between NO- 3 and Cl^- ($R^2 = 0.479$). With constant exacerbation of soil salinization, nitrates in soil-soluble salts increased with Cl^- concentrations. Soils with the highest NO_3^- content (up to 2.27 mmol/L) were distributed near the coastal zone. This may be related to fish farming in the study area. In contrast, the NO_3^- content in groundwater varies by a large degree, ranging from 0.02 to 11.78 mmol/L (Table 2); there was no positive correlation between NO_3^- and Cl^- in groundwater. The highest NO_3^- concentration occurred groundwater with a Cl^- concentration of 45–50 mmol/L; this sample was collected at a location representative of agricultural areas that experience the excessive

use of fertilizer (Fang *et al.* 2006). Saline water with high Cl^- concentrations had low NO_3^- concentrations; this pattern has previously been confirmed as a consequence of seawater intrusion (Park *et al.* 2005).

The Cl/Br ratios were also used to estimate the origin of groundwater salinity (Cartwright *et al.* 2006). The Cl/Br molar ratio would be approximately 655 if Cl^- and Br^- in groundwater originated from seawater (Siemann 2003). Figure 5(f) shows the Cl^- concentrations as a function of Cl/Br in groundwater and soil samples. Molar Cl/Br ratios in groundwater samples with low salinity (Cl^- <36 mmol/L) varied considerably, ranging from 178 to 1,834. The highest Cl^-/Br^- ratios of up to 1,834 occurred in groundwater with Cl^- concentrations of 27 mmol/L. However, Cl^-/Br^- ratios of halite are commonly from 10^4 to 10^5, and groundwater salinization in low salinity was understood to be influenced by halite dissolution in the aquifer (Cartwright *et al.* 2006). The range for the Cl^-/Br^- ratios in 11 soil samples (the remaining samples were below the detection limit of bromine) with high Cl^- concentrations was between 345 and 1,187, with a mean of 783. All soil samples were also unsaturated with respect to halite, with SI_{Halite} between –8.32 and –3.56 (Figure 6(d)), as the evaporation process did not alter the Cl^-/Br^- ratios until halites were saturated. However, the dissolution of halite increased the Cl^-/Br^- ratios and Cl^- concentrations. Based on the results of this analysis, the mechanisms that underpin the regulation of salt accumulation in groundwater and soil is either the evaporation of relict seawater or the mixing of recent seawater, as opposed to halite dissolution.

Cation exchange

Cation exchange is a hydrogeochemical process that frequently occurs in the groundwater of coastal areas (Cruz & Silva 2000), and is one of the contributors to soil salinity. This study used two chloro-alkaline indices $CAI_1 = [c(Cl^-) - c(Na^+ + K^+)]/cCl^-$ and $CAI_2 = [c(Cl^-) - c(Na^+ + K^+)]/[2c(SO_4^{2-}) + c(HCO_3^-) + c(NO_3^-)]$, that suggested that ion exchange occurred between Na^+ in the soil solution, and Ca^{2+} or Mg^{2+} in weathered materials (Schoeller 1965). It was anticipated that both indices would be positive when Na^+ in groundwater is exchanged for Ca^{2+} or Mg^{2+} in sediment or soil (backward reaction). Otherwise, Ca^{2+} or Mg^{2+} in the target solution is exchanged for Na^+ in the sediment or soil (forward reaction).

Figure 7 illustrates a weak trend of decreasing CAI1 and CAI2 with increasing distance. In the study area, soil samples with 85% of CAI1 and 90% of CAI2 greater than 0 were preferentially located within 40 km of the coastline. Almost 100% of the CAI1 and CAI2 were negative for soil samples that were 80 km away from the coastline. These values suggest that soil cation exchange is more likely to occur in close proximity to the sea.

Soil salinization with seawater mixing

Based on the computation methods by Sinclair (1974), the following threshold values (T) were estimated: $Cl^- = 2{,}710$ mg/L, $SO2- 4 = 660$ mg/L, $Na^+ = 1{,}280$ mg/L, $Mg^{2+} = 320$ mg/L (Figure 8). The SMI was calculated for each groundwater sample using Equation (1); Figure 9 shows the SMI distribution and the degree of soil salinization in the study area. Generally, soil salinity had become aggravated with an increase in SMI. All non-salinized soil samples and 85% of soil samples with mild salinization were located in areas with an SMI less than 1. However, 80% of soil samples with moderate salinization and all severely salinized soil samples were scattered in saline water or brine regions, with groundwater SMI exceeding 1. The groundwater in this area was significantly affected by the mixing of seawater components (Park *et al.* 2005; Mondal *et al.* 2011). Therefore, the exacerbation of soil

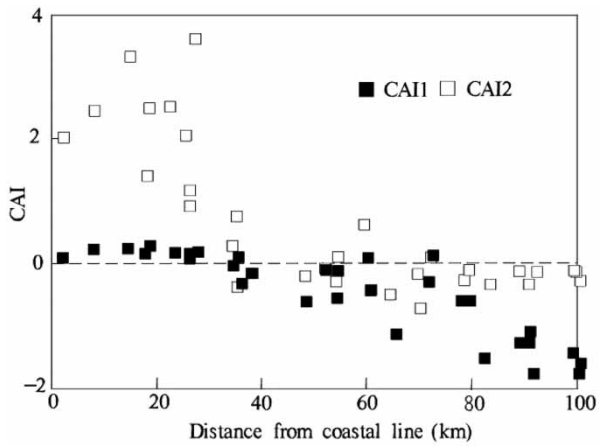

Figure 7 | Relationships between the distance from the coast and CAI1 and CAI2 in soil.

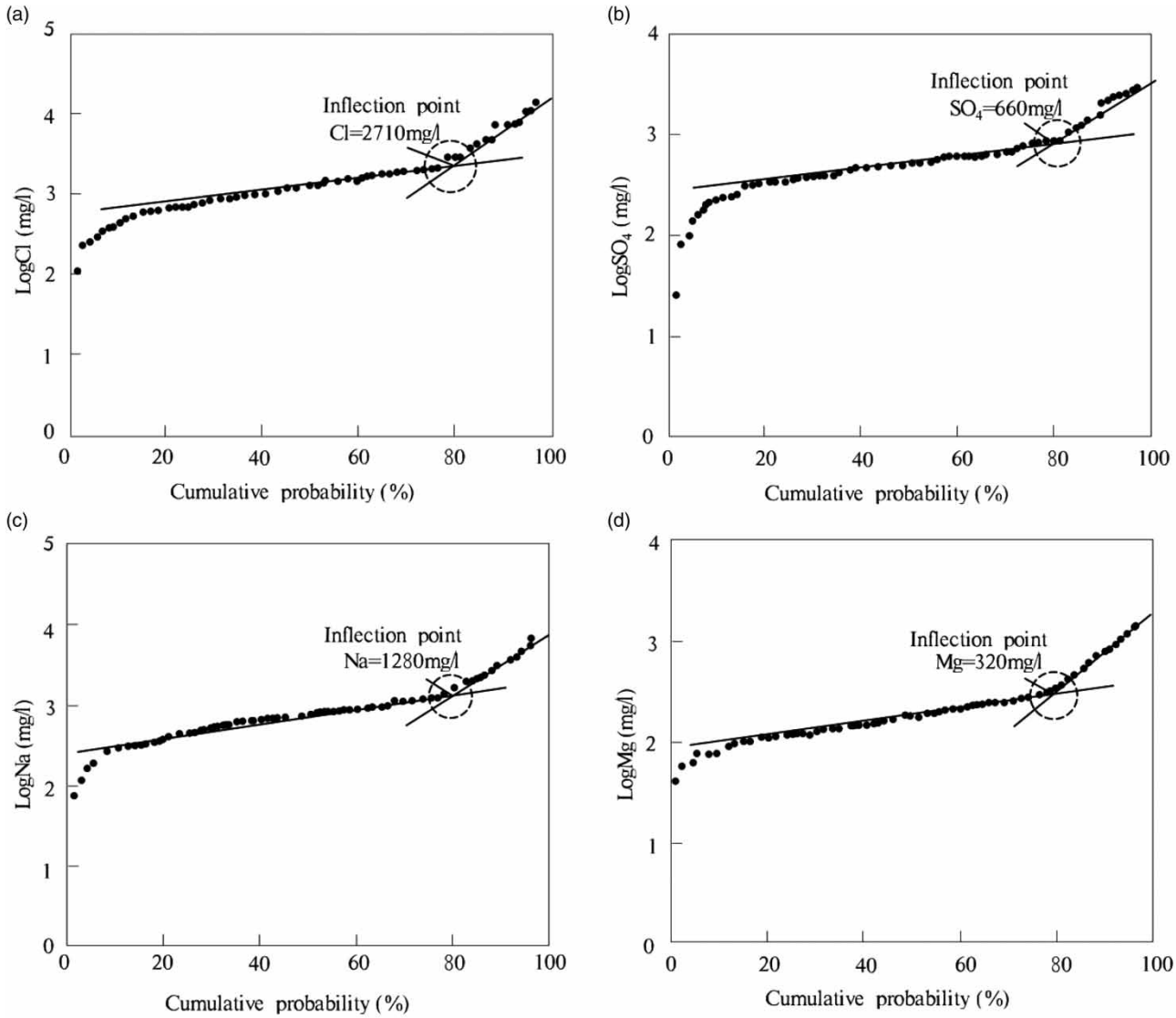

Figure 8 | Cumulative probability curves for concentrations of (a) Cl^-; (b) SO_4^{2-}; (c) Na^+; and (d) Mg^{2+} in groundwater. The estimation of inflection points (corresponding to regional threshold values) is based on Sinclair (1974).

salinization was a result of increasing groundwater salinity with ongoing mixing with seawater.

Soil salinity and groundwater evaporation

The evaporation of shallow groundwater is a key factor underlying soil salinization. The plot of $\delta^{18}O$ versus Cl^- in groundwater reveals that the evolution of shallow groundwater proceeded in three distinct phases (Figure 10). First, when the Cl^- concentration was between 10 and 30 meq/L, $\delta^{18}O$ only varied slightly from −9.08 to −6.87‰. This was not correlated with Cl^-, as evaporite dissolution increases Cl^- concentration, and does not impact on stable isotopes. As such, evaporite dissolution is considered to have occurred during groundwater evolution at lower Cl^- concentrations. Second, the increasing Cl^- concentration was slightly positively correlated with $\delta^{18}O$ in partial groundwater samples, implying that seawater mixing had a marginal effect on groundwater salinity. Lastly, when $Cl^- > 100$ meq/L, strong evaporation had shifted the $\delta^{18}O$ in groundwater to be 4.17–11.79‰, which is higher than zero and even more than that of seawater. This

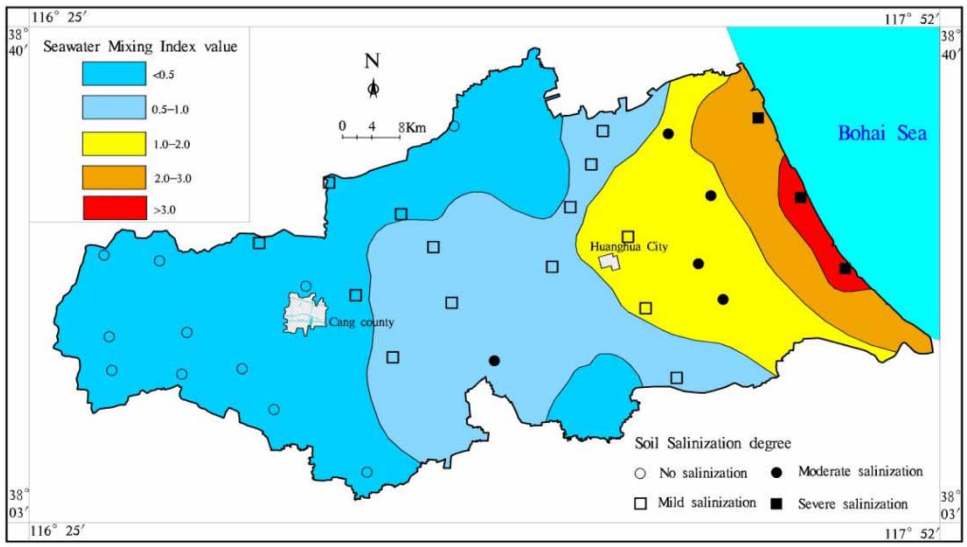

Figure 9 | The spatial distribution of the seawater mixing index (SMI) and degree of soil salinization. The latter was classified according to salt content (Table 1).

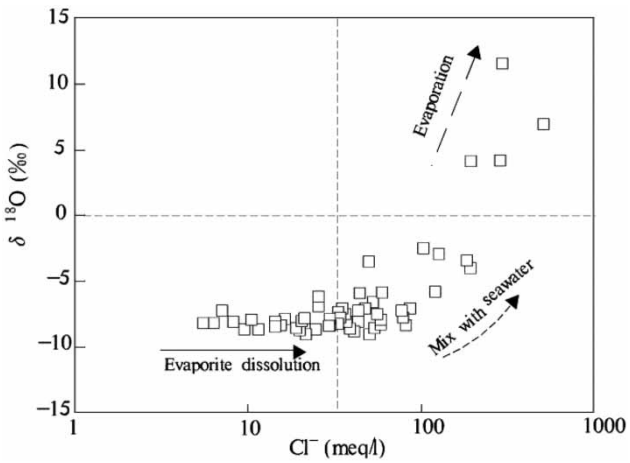

Figure 10 | Plots of $\delta^{18}O$ versus Cl^- in groundwater. The evolution of groundwater was roughly divided into three stages: evaporite dissolution, seawater mixing, and remnant seawater evaporation.

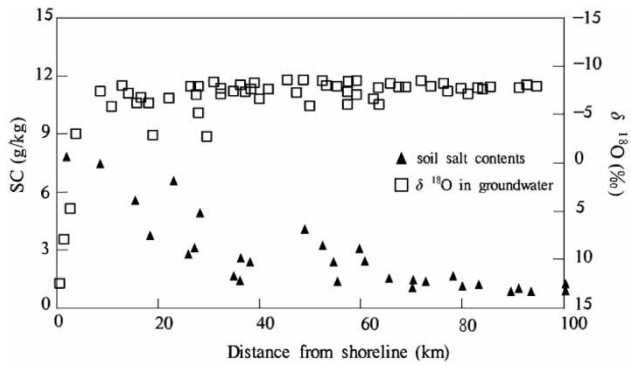

Figure 11 | Plots of $\delta^{18}O$ in groundwater and soil salinity versus distance from coast.

phenomenon often occurs in brine as a result of the evaporation of remnant seawater (Vengosh *et al.* 1999).

The relationships between $\delta^{18}O$ in groundwater, soil salinity, and distance from the coastal line are shown in Figure 11. In the plot, the $\delta^{18}O$ of groundwater and soil salinity decreased with distance from the sea. When the sampling point distance to the coastline was greater than 40 km, there was low variation in soil salinity in different soils and $\delta^{18}O$ in groundwater, ranging from 2 to 4 g/kg and −9.08 to −6.18‰, respectively. With increasing proximity to the sea, soil salinity showed a stronger enrichment than that of $\delta^{18}O$, increasing at distances of 20 and 40 km. Strong evaporation with shallow groundwater depth plays a major role in governing soil salinity near the coastline. Soil salinity reaches severe salinization (SC > 6 g/kg), and the $\delta^{18}O$ values in groundwater exceed zero, demonstrating intense enrichment.

Conceptual model of groundwater salinization process controlling the soil salinity

The results of this study provide a basis for a unifying conceptual model that describes groundwater hydrochemical processes and their influence on soil salinization along a

cross-section, from inland areas to coastal areas (Figure 12). The regional soil salinity distribution was affected by groundwater hydrogeochemical processes. These processes may be roughly divided into three stages. First, with considerable distance from coastal areas, shallow groundwater with TDS < 3 g/L and more negative $\delta^{18}O$ experiences the continental salinization process. As the groundwater table in these areas are typically deep, it enhances the effect of rain leaching and led to a reduction in soil salinity with no-salinization or mild-salinization levels. Second, with increasing proximity to the sea, shallow groundwater is gradually affected by seawater mixing, evolving into saline water with a TDS between 3 and 10 g/L and a Cl–Na type. The wide range of $\delta^{18}O$ and the CAI1 and CAI2 values exceeding zero suggest that strong evaporation and ion exchange of Ca for Na in soil primarily causes salt accumulation in soils. Lastly, soil salinity deteriorates to severe-salinization levels as a result of seawater intrusion close to the coastline. In this instance, soil salinity is directly affected by seawater evaporation in the presence of an extremely shallow water table. The Cl^-/Br^- ratios and positive $\delta^{18}O$ of the groundwater indicates that relict seawater were the main sources of salt.

CONCLUSIONS

Soil salinization is one of the most widespread environmental problems in coastal areas. Cangzhou City is a typical coastal area in northern China, where soil degradation has been observed since the 1950s. Understanding the origin and evolution of soil salinity is critical to improve land production capacity and utilize soil resources reasonably.

This study used groundwater hydrochemical and isotopic data to characterize the impact of groundwater hydrochemical processes on soil salinization. Groundwater evaporation and sea intrusion were identified as the predominant factors for soil salinization. Non-salinization and mild salinization occurred in soils located to the west of Cang County; these soils were located at a considerable distance from the sea. The low TDS of groundwater and the deep water table restricted the upward trajectory of soil

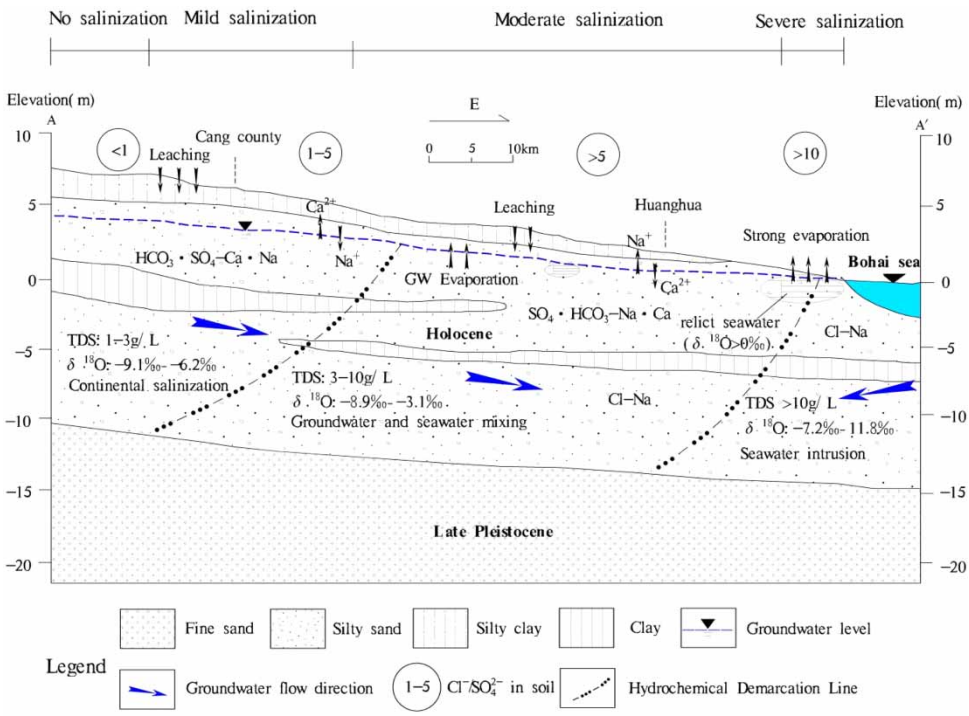

Figure 12 | Conceptual model of soil salinity under the control of groundwater salinization. Geologic cross-section of the location in Figure 1.

salinity in this region. Along the water flow direction, the SC in groundwater had gradually increased via seawater mixing, accumulating on the soil surface soil. Cation exchange intensified soil alkalization with moderate salinization. High NO_3^- concentrations in soil occurred in the east of the study area, suggesting that nitrogen fertilizer was a non-negligible source of soil salinity in agricultural areas. Areas with severe salinization and brine water were located to the east of Huanghua City, near the coastal area. The particular Cl^-/Br^- ratios and high content of $\delta^{18}O$ and δ^2H indicate that relict seawater evaporation was the main source of salt in the soil. The results of this study provide insights into the origin of soil salinization in this coastal region, which may be applicable to other similar coastal regions.

ACKNOWLEDGEMENT

This work was supported by the China Geological Survey (CGS) grant No. DD20190259 'Comprehensive geological survey of northern Taihang mountains' and grant No. 12120113103300 'Hydrogeological survey of typical saline-alkali areas in the central Hebei Plain'. The authors would like to thank Dr Wang and two other anonymous reviewers for their instructive suggestions, which significantly improved the original manuscript.

DATA AVAILABILITY STATEMENT

All relevant data are included in the paper or its Supplementary Information.

REFERENCES

Cartwright, I., Weaver, T. & Fifield, L. 2006 Cl/Br ratios and environmental isotopes as indicators of recharge variability and groundwater flow: an example from the southeast Murray Basin, Australia. *Chem. Geol.* **231**, 38–56. doi:10.1016/j.chemgeo.2005.12.009.

Chen, Z., Qi, J., Xu, J., Xu, J., Ye, H. & Nan, Y. 2003 Paleoclimatic interpretation of the past 30 ka from isotopic studies of the deep confined aquifer of the North China plain. *Appl. Geochem.* **18** (7), 997–1009. doi:10.1016/S0883-2927(02)00206-8.

Chen, J., Han, S. & Xiao, W. 2018 Study on spatio-temporal changes and rehabilitation of Saline-Alkali Land in the Coastal Area of Cangzhou. *Nat. Resour. Econ. China* **31** (11), 38–39. doi:10.19676/j.cnki.1672-6995.0000124. (in Chinese).

Cruz, J. & Silva, M. 2000 Groundwater salinization in Pico Island (Azores, Portugal):origin and mechanisms. *Environ. Geol.* **39**, 1181–1189. doi:10.1007/s002540000109.

Fang, Q., Yu, Q., Wang, E., Chen, Y., Zhang, G., Wang, J. & Li, L. 2006 Soil nitrate accumulation, leaching and crop nitrogen use as influenced by fertilization and irrigation in an intensive wheat-maize double cropping system in the North China Plain. *Plant. Soil* **284**, 335–350. doi:10.1007/s11104-006-0055-7.

Ghassemi, F., Jakeman, A. J. & Nix, H. A. 1995 Salinisation of land and water resources: Human causes, extent, management and case studies. In *Centre for Resource and Environmental Studies*, Canberra, Australia.

Han, D., Vincent, E. A. P. & Song, X. 2015 Groundwater salinization processes and reversibility of seawater intrusion in coastal carbonate aquifers. *J. Hydrol.* **531**, 1067–1080. doi:10.1016/j.jhydrol.2015.11.013.

Li, Y. 1994 Mass balances of major chemical constituents in Bohai Sea water II. Removal processes. *Chin. J. Oceanol. Limnol.* **12** (3), 236–245. doi:10.1007/BF02845169. (in Chinese).

Liu, X. 2018 Reclamation and utilization of saline soils in water-scarce regions of Bohai Sea. *Chin. J. Eco-Agric.* **26** (10), 1521–1527. doi:10.13930/j.cnki.cjea.180725. (in Chinese).

Lu, Z., Yang, J., Liu, G., Li, J., Liu, H. & Li, B. 2017 Relationship between soil salinization and groundwater characteristics in the Yellow River Delta. *Acta Pedological. Sinica* **54** (6), 1377–1385. doi:10.11766/trxb201701160401. (in Chinese).

Mondal, N., Singh, V., Singh, S. & Singh, V. 2011 Hydrochemical characteristic of coastal aquifer from Tuticorin, Tamil Nadu, India. *Environ. Monit. Assess.* **175**, 531–550. doi:10.1007/s10661-010-1549-6.

Neal, C. & Kirchner, J. W. 2000 Sodium and chloride levels in rainfall, mist, streamwater and groundwater at the Plynlimon catchments, midwales: inferences on hydrological and chemical controls. *Hydrol. Earth. Syst. Sc.* **4** (2), 295–310. doi:10.5194/hess-4-295-2000.

Park, S., Yun, S., Chae, G., Yoo, I., Shin, K., Heo, C. & Lee, S. 2005 Regional hydrochemical study on salinization of coastal aquifers, western coastal area of South Korea. *J. Hydrol.* **313** (3–4), 182–194. doi:10.1016/j.jhydrol.2005.03.001.

Schoeller, H. 1965 *Hydrogunamique dans le karst (Hydrogynamics of karst)*. Actes du Colloques de Doubronik. IAHS/UNESCO, Wallingford, pp. 3–20.

Siemann, M. 2003 Extensive and rapid changes in seawater chemistry during the Phanerozoic: evidence from Br contents in basal halite. *Terra. Nova.* **15**, 243–248. doi:10.1046/j.1365-3121.2003.00490.x.

Sinclair, A. 1974 Selection of threshold values in geochemical data using probability graphs. *J. Geochem. Explor.* **3**, 129–149. doi:10.1016/0375-6742(74)90030-2.

Uma, S. 2013 Relationship between groundwater properties and soil salinity at the Lower Nam Kam River Basin in Thailand. *Environ. Earth. Sci.* **69**, 1803–1812. doi:10.1007/s12665-012-2012-5.

Vengosh, A., Spivack, A. J., Artzi, Y. & Ayalon, A. 1999 Geochemical and boron, strontium, and oxygen isotopic constraints on the origin of the salinity in groundwater from the Mediterranean Coast of Israel. *Water. Resour. Res.* **35** (6), 1877–1894. doi:10.1029/1999WR900024.

Wang, G., Fang, Q., Wu, B., Yang, H. & Xu, Z. 2015a Relationship between soil erodibility and modeled infiltration rate in different soils. *J. Hydrol.* **528**, 408–418. doi:10.1016/j.jhydrol.2015.06. 044.

Wang, W., Li, G., Hou, J. & Liu, Y. 2015b Salinization characteristics of soil profile in coastal areas of Tianjin and its affecting factors. *Geophys. Geochem. Explor.* **39** (1), 172–179. doi:10.11720/wtyht.2015.1.28. (in Chinese).

Wang, J., Wu, J. & Jia, H. 2016 Analysis of spatial variation of soil salinization using a hydrochemical and stable isotopic method in a semiarid irrigated basin, Hetao Plain, Inner Mongolia, North China. *Environ. Process.* **3** (4), 723–733. doi:10.1007/ s40710-016-0179-6.

Zhang, Z., Shen, Z., Xue, Y., Ren, F., Shi, D., Yin, Z., Zhong, Z. & Sun, X. 2000 *Groundwater Environmental Evolution in North China Plain*. Geology Press, Beijing, China. (in Chinese).

Zhou, Z. & Zhao, S. 2015 Influencing factors on surface soil salt accumulation in the semi-arid North China Plain. *Arid. Land Geogr.* **38**, 976–984. doi:10.13826/j.cnki.cn65-1103/x.2015.05.012. (in Chinese).

Zhou, Z., Zhang, G., Yan, M. & Wang, J. 2012 Spatial variability of the shallow groundwater level and its chemistry characteristics in the low plain around the Bohai Sea, North China. *Environ. Monit. Assess.* **184** (6), 3697–3710. doi:10.1007/s10661-011-2217-1.

First received 14 December 2020; accepted in revised form 1 February 2021. Available online 10 March 2021